Design and Implementation of Neuro-Fuzzy Controller Using FPGA for Sun Tracking System

Ammar A. Aldair
Electrical Eng.
University of Basrah
Basra/ Iraq.
mmr.ali2@gmail.com

Adel A. Obed
Electrical Power Eng.
Middle Technical University
Baghdad/ Iraq.
adelrazan@yahoo.com

Ali F. Halihal
Electrical Eng.
University of Basrah
Basrah/ Iraq.
ali_fadheel@yahoo.com

Abstract

Nowadays, renewable energy is being used increasingly because of the global warming and destruction of the environment. Therefore, the studies are concentrating on gain of maximum power from this energy such as the solar energy. A sun tracker is device which rotates a photovoltaic (PV) panel to the sun to get the maximum power. Disturbances which are originated by passing the clouds are one of great challenges in design of the controller in addition to the losses power due to energy consumption in the motors and lifetime limitation of the sun tracker. In this paper, the neuro-fuzzy controller has been designed and implemented using Field Programmable Gate Array (FPGA) board for dual axis sun tracker based on optical sensors to orient the PV panel by two linear actuators. The experimental results reveal that proposed controller is more robust than fuzzy logic controller and proportional-integral (PI) controller since it has been trained offline using Matlab tool box to overcome those disturbances. The proposed controller can track the sun trajectory effectively, where the experimental results reveal that dual axis sun tracker power can collect 50.6% more daily power than fixed angle panel. Whilst one axis sun tracker power can collect 39.4 % more daily power than fixed angle panel. Hence, dual axis sun tracker can collect 8 % more daily power than one axis sun tracker.

Index Terms— **Dual axis sun tracker, Field Programmable Gate Array (FPGA), Neuro-fuzzy controller, Optical sensors**

I. INTRODUCTION

In 1962, the first sun tracker introduced by Finster, was completely mechanical. After that, Saavedra proposed a mechanical structure with an electronic circuit to control an Eppley pyrheliometer orientation [1].

The solar tracker is a device which orients Photovoltaic (PV) panel where it is perpendicular to the sunlight throughout day. The solar tracking system is used to improve the efficiency of the PV panel by tracking the sun. Presence of a solar tracker is not essential for the operation of a solar panel, but without it, performance is reduced. In general, the dual axis sun tracker allows solar panel to collect up to 50% more energy than that can be collected using stationary solar panels.

However, there are many problems in sun tracker installation such as energy consumption in its components, periodic maintenance, cost,

reliability and performance must be taken into the account [1,2].

Many projects and researches are noted that focus on intelligent controller in the optical sensor based sun tracker.

B. Hamed and M. EL-Moghany [3] designed and implemented fuzzy logic controllers via Field Programmable Gate Array (FPGA) to control one axis sun tracker. They used stepper motor to improve accuracy of the sun tracker. The proposed sun tracker and MPPT controllers are tested by Matlab/Simulink program, the results show that controllers have a good response.

B. Hamed and K. El-Nounou [4] designed Sugeno fuzzy logic controller which is used to increase the energy generation efficiency of solar cells by one axis sun tracker which is driven by stepper motor and. Genetic Algorithm (GA) has been employed to optimize the input memberships, inputs gain and output gain of the fuzzy logic controllers. The proposed sun tracker controller is tested using Matlab/Simulink

program, the results show that the Sugeno controller has a good response when compared with Mamdani controller.

Hanan A. R. Akkar and Yaser M. Abid [5] proposed intelligent dual sun tracker controller which implemented on FPGA with 4 LDRs and two DC motors. The proposed controller is neural network which is trained by two ways: supervised feed forward neural network and particle swarm optimization (PSO). The simulation results reveal that supervised feed forward neural network is better training than PSO. The experimental results reveal that the proposed controller for dual sun tracker increases energy gain 44.3 % of the PV system compared with stationary panel.

The apparent motion of the sun in the sky is because of two effects:

- Daily rotation of the Earth around its axis.
- The tilt of the Earth on its axis of rotation that due to seasonal variation. This tilt is described by the declination angle (δ).

The declination angle is the angle between the plane of the earth 's equator and a line drawn from the sun center to the earth center. It varies from -23.45^o at 22 December, 0° at 21 March and 21 September, to 23.45^o at 21 June.

The declination angle can be calculated by:

$$\delta = 23.45^o \sin(\frac{360}{365}(d + 284)) \qquad (1)$$

where d is the number of the day of the year with 1 January as $d = 1$ [6].

The hour angle (ω) describes the instantaneous position of the sun and is the angle between the sun's direction and the solar noon. This angle varies 1° every 4 minutes or 15° every hour and is given as:

$$\omega = 15^o (h - 12) \qquad (2)$$

where h is the hour considered (24 hour clock). Thus, In the morning, ω is negative, at the solar noon, ω is zero, the afternoon, ω is positive.

For display and logging of data from the PV system, the graphical user interface (GUI) has been programmed using visual basic 2008 as indicated in Figure 1.

II. COMPONENTS OF THE PROPOSED SUN TRACKING SYSTEM

In the present work, the main components of the solar tracking system are: FPGA board, analog to

digital converter integrated circuit, mechanical parts, linear actuators, driver motors and photo sensors. There are two independent systems, the first system is the polar axis sun tracker and the second system is the tilt axis sun tracker.
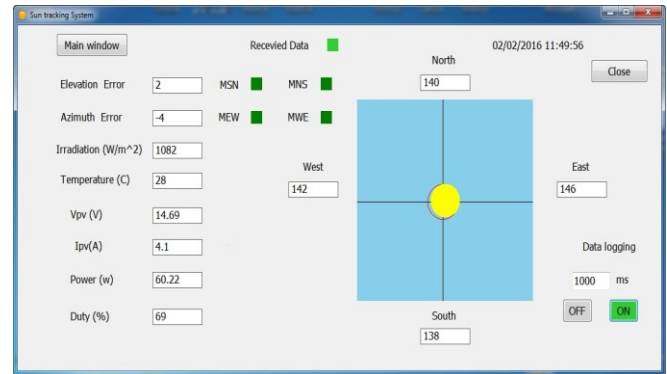

Figure 1: The GUI of the sun tracking system

The polar axis sun tracker consists of the west and east photo sensors and the FPGA board, the driver motor and the polar axis linear actuator are shown in Figure 2.

In this tracker, the FPGA computes the error as a difference between the reading of west and east photo sensors. The error summation is calculated from the sum of ten past samples of the error (sampling period is 1 second). The error and the error summation signals are applied as input to PI like neuro-fuzzy controller and the output of the controller is compared inside the FPGA with positive maximum threshold (+max), negative maximum (-max) threshold, positive minimum (+min) threshold and negative minimum (-min) threshold as shown in Figure 3. The comparison results (If statements) determine stopping or rotation of the PV panel toward the west or the east by the motor driver and the linear actuator.
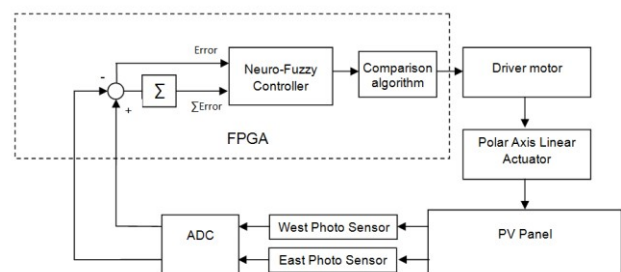

Figure 2: Block diagram of polar axis sun tracker

The tilt axis sun tracker is similar to the polar axis sun tracker except the north and south photo

sensors are existed instead of the west and east photo sensors, and the tilt axis linear actuator is located instead of the polar axis linear actuator as shown in Figure 4.
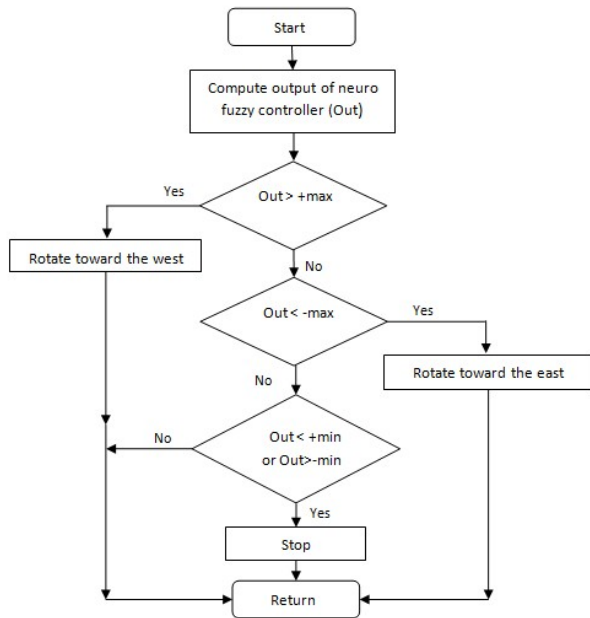

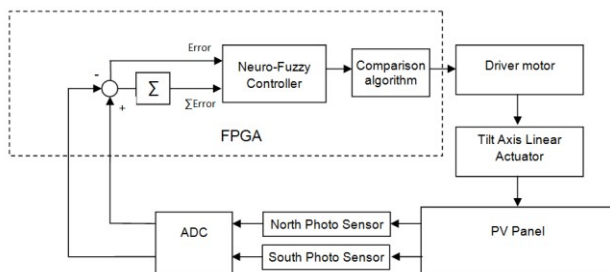Figure 3: Flow chart of the comparison algorithm for the proposed sun tracker controller

Figure 4: Block diagram of tilt axis sun tracker

The major components of the solar tracking system are:

A. FPGA Board
It is one common kind of programmable logic devices (PLDs). It is an integrated circuit which a designer or a user is able to configure it after manufacturing. The FPGA consists Configurable Logic Blocks (CLBs), Input-Output Blocks (IOBs) and Programmable Interconnect Resources (PIRs) which allow the blocks to be connected together, like several electronic circuits which can be inter-wired in different topologies or configurations [7]. A CLB consists of a few logical cells (called Adaptive Logic Modules (ALM), logic Elements (LE), Slice etc).

The logic blocks that make up the bulk of the device are based on Look-Up Table (LUT) combined with one or two single-bit registers (flip-flop) and additional logic elements such as clock enables and multiplexers [7].

The advantage of a controller implemented by FPGA includes shorter development cycles, lower cost, small size, fast system execute speed, and high flexibility.

The FPGA-EP4CE6E22C8N device has been used to build neuro-fuzzy controller as indicated in Figure 5. It is a device from the Cyclone IV-E devices family which manufactured by Altera Corporation.

The key features for this device are [8]:

1) 6272 Logic elements (LEs).

2) 270 Kbits embedded memory.

3) 15 embedded 18×18 multipliers.

4) 2 general-purpose phase-locked loops (PLLs).

5) 10 global clock networks.

6) 92 user input/output pin out.

The neuro-fuzzy controller implementation consumed 5141 LEs, 484 registers and 14 embedded 18×18 multipliers inside the FPGA.

The FPGA uses static random access memory cells to store configuration data. It is downloaded to the FPGA each time, the device restarts.

B. Analog to Digital Converter (ADC)
Since the used FPGA board deals with just digital signals, while, most of the field signals are analog type, it is essential that the analog to digital converter is used. The neuro-fuzzy controller for the sun tracker requires four analog input signals. Fortunately, Integrated circuit ADC0808 also has eight channels. Integrated circuit ADC0808 components are monolithic CMOS device with an 8-bit analog to digital converter and 8-channel multiplexer. The 8-bit A/D converter always uses successive approximation as the conversion technique [9].

The key features for ADC0808 are:
1) 8 bit resolution.
2) 100 µs conversion time.
3) ±1 LSB maximum error .

Figure 6 illustrates connection diagram of ADC0808CCN device.

An ADC0808 contains eight channels which are single ended. The analog Input channel is selected by the address of the multiplexer.
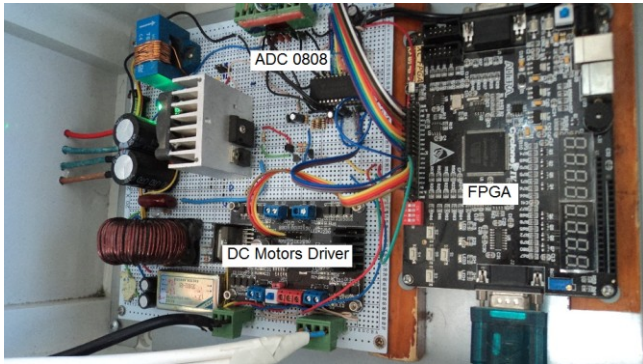

Figure 5: The FPGA, DC motors driver and ADC0808 implementation

Figure 6 illustrates the hardware controller that consists of FPGA-EP4CE6E22C8N device, ADC0808, motor drivers (polar and tilt) and buck converter. There are four types of lines which are used to interface between the ADC and the FPGA:

1) 8 bit digital outputs lines (From B_7 to B_0).

2) Addresses input lines (ADD C,ADD B,ADD A).
3) Clock line.
4) Start and address latch enable (ALE) lines.

The clock frequency that has generated by the FPGA is 500 kHz. The process reading of the analog signals can be explained as follow:

1. The FPGA outputs specific address lines for channel IN0.
2. The FPGA generates the conversion starting pulse with width equal to 2 μs. successive approximation register is reset on transition from 0 to 1 of the start conversion pulse. The conversion is started on transition from 1 to 0 of the start conversion pulse.
3. After conversation time equal to100 μs, the FPGA reads 8-bits digital output.
4. Above steps repeats for next channels till attain to channel IN7,then to channel IN0 again. Thus, the process continues.

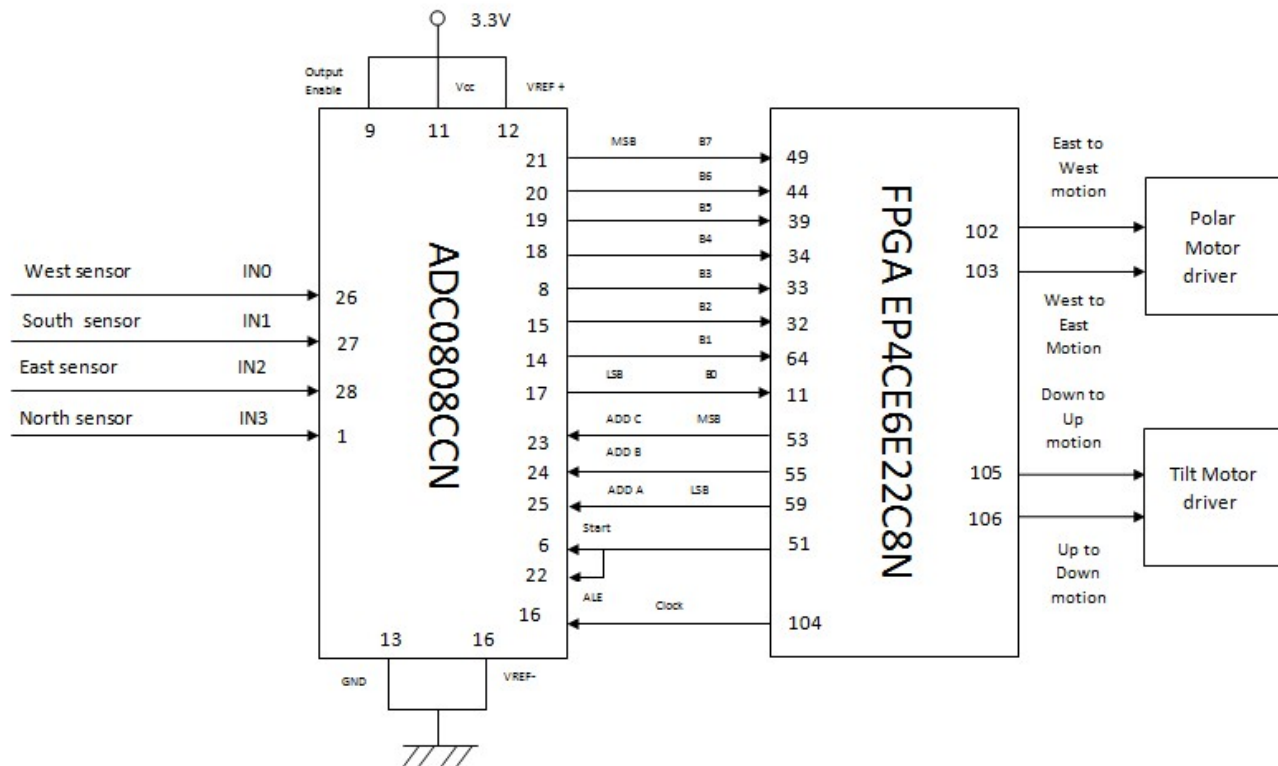The time cycle for 8 channels reading has been selected as 2.5 ms.

Figure 6: Block diagram for the hardware controller

C. *The Mechanical Parts*

The mechanical system is two degrees of freedom to change the direction of SR-60S 60W PV module to track the sun light in the two directions. Figure 7 shows the main mechanical parts of our model which are listed below:-

1) Solar mounting arms to carry the PV module.
2) Main tracker mount that is attached to the solar mounting arms.
3) Post that is attached to the main tracker mount. This post must be faced exactly south, if it lies in the northern hemisphere. While, it must be faced exactly north if it lies in the southern hemisphere. In addition, it must be perpendicular on the earth's surface.

D. *Linear Actuator*

The linear actuator used in the present work is DC permanent magnet motor with worm gear and stroke length is 450 mm as shown in Figure 8.

There are two linear actuators; the first one is used to rotate the PV module to face the sun towards horizontal or west/east direction. While, the other one is used to rotate the module to face the sun towards vertical or north/south direction.

The linear actuator speed is 5mm/s. So, the solar panel rotates at 1 degree/s average angular speed. The motor voltage is 24V and it draws 0.3A current at steady state. The starting current (0.66A) can be neglected because the starting time (80ms) is short with respect to the turn on time (5s). So, the rated consumed power is 7.2W. Therefore, it must be taken into the account that this power reduces the efficiency of the system.

Linear actuator contains two limit switches and two diodes. A limit switch is used to determine a position of the module to prohibit the impact when it reaches the terminals.
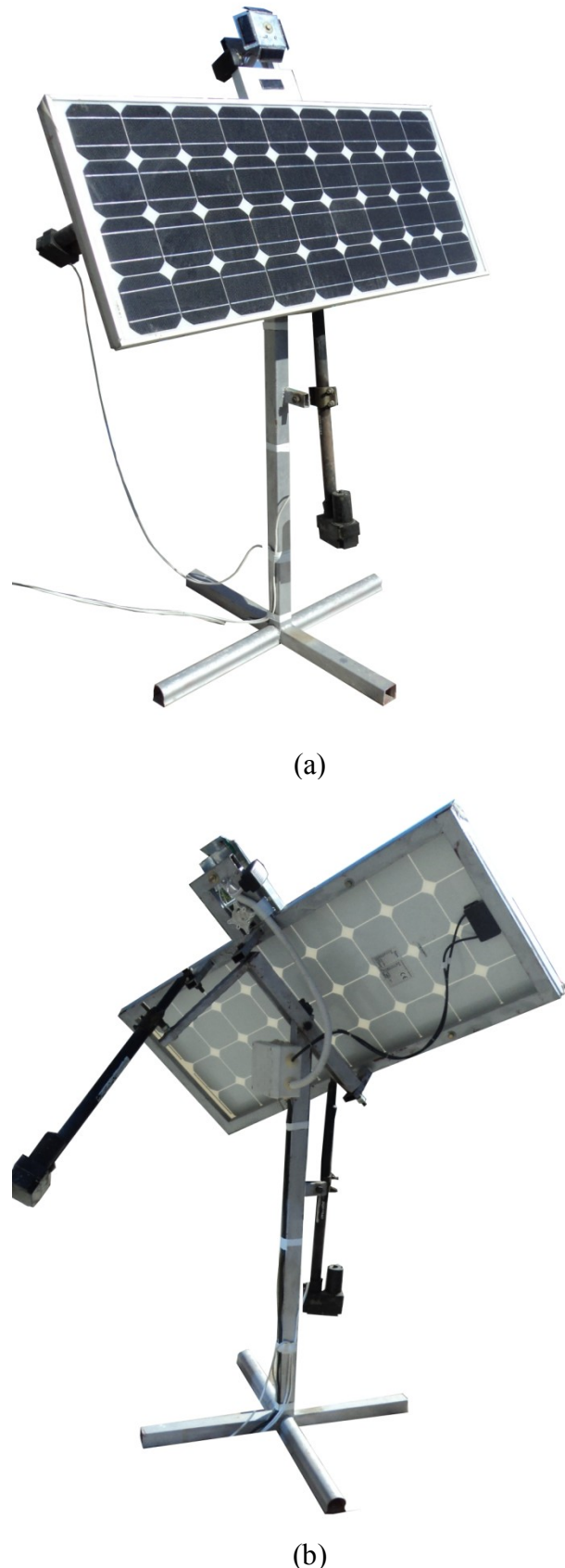
(a)

(b)

Figure 7: The mechanical system of the sun tracker: (a) Front view and (b) Back view

Figure 8: Linear actuator

Figure 9 indicates connection these limit switches and diodes with motor. This topology is configured to the left limit switch is open when the module reach to the one the specific terminal as east, the reverse voltage allows to apply to motor by the left diode.
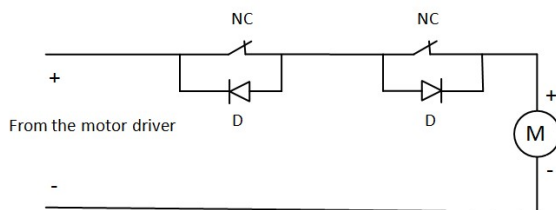

Figure 9: The electric circuit of the linear actuator

E. The Motor Driver

Each linear actuator is controlled by the motor driver module. The module contains two integrated circuit L298 that is dual full bridge driver. In general, it is designed to drive inductive loads as solenoids, relays, stepping and DC motors.

In the present work, the motor driver is used to control the direction of two DC motors since it has high current and high voltage. For each motor, the two input signals come from FPGA pins, the first signal is used to rotate the motor

clockwise direction, whilst the other signal is used to rotate the motor counter clockwise. The output of the motor driver module is connected to motor and the voltage supply is 24V. Figure 10 illustrates the motor driver module.
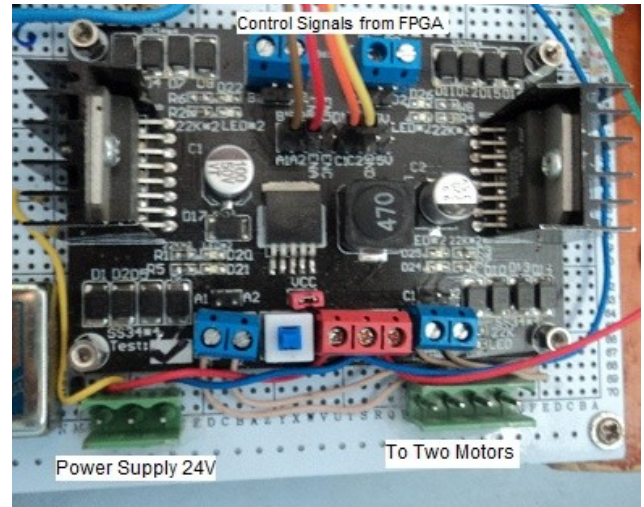

Figure 10: The driver motor module connection

F. The Photo Sensors

In this work, the sun tracker has two axis tilt-polar (equatorial) trackers. Therefore, four small PV modules are used as a photo sensor. Each axis has two identical sensors. In other word, the polar axis has west and east photo sensors, whilst tilt axis has north and south photo sensors as shown in Figure 11. Each photo sensor is connected to ADC 0808 channel across 49.5 Ω resistor in order to convert the current generated by the sensor to the voltage.
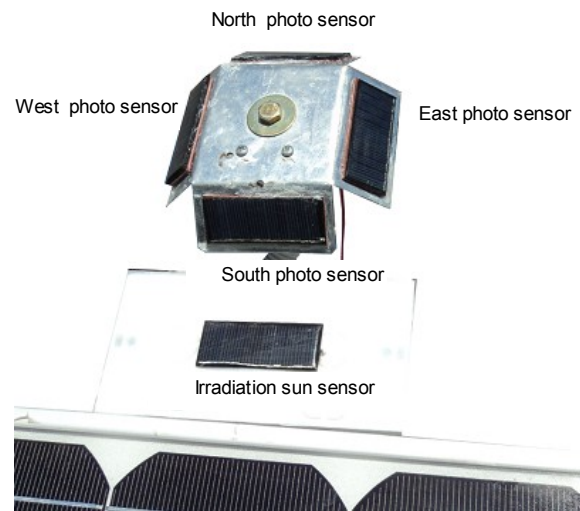

Figure 11: Four photo sensors implementation

III. MATHEMATICAL MODEL OF THE PROPOSED PHOTO SENSORS SYSTEM

The misalignment angle (θ) may be defined as the angle between the sunlight beam and the panel normal as shown in Figure 12. This angle may be composed from two angles, the horizontal misalignment angle (θ_h) where west and east photo sensors are responsible for measure the amount of this angle; and the vertical misalignment angle (θ_v) where north and south photo sensors are responsible for measure the amount of this angle. In the present work, the sun position measurement is based on shade balancing principle tilted mount of photo sensors as indicated in Figure 13. It can be seen clearly in this Figure, the incident intensity of light on west photo sensor (G_{ws}) is given by:

$$G_{WS} = G\cos(45^o - \theta_h) \qquad (3)$$

where G is solar irradiation (W/m^2).
Also, the incident intensity of light on east photo sensor (G_{ES}) is given by:

$$G_{ES} = G\cos(45^o + \theta_h) \qquad (4)$$

The controller computes the horizontal error of irradiation (Err_h) from difference between signals of west and east photo sensors, which is given by:

$$Err_h = G_{WS} - G_{ES} \qquad (5)$$

Therefore, by combining Equations (3-5), Err_h becomes:

$$Err_h = G\left[\cos(45^o - \theta_h) - \cos(45^o + \theta_h)\right] \qquad (6)$$
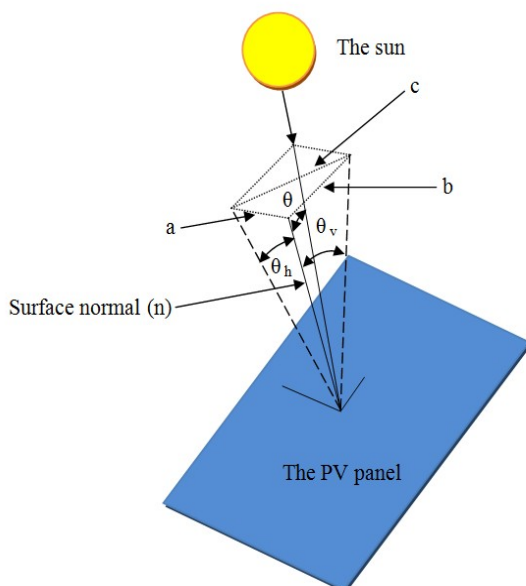

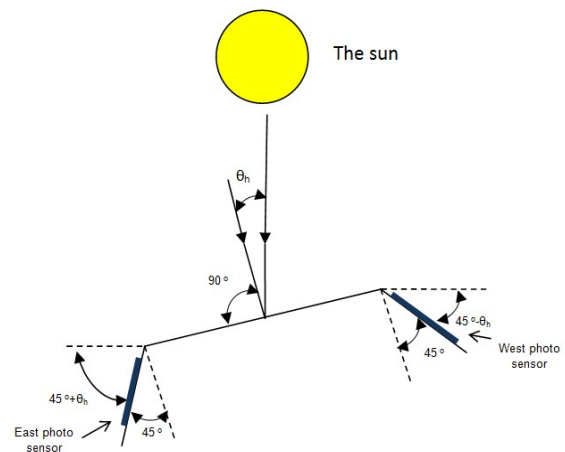Figure 12: Compounds of the misalignment angle

Figure 13: The sun position measurement based on shade balancing principle

In mathematics, sum and difference two angles identities is given by:

$$\cos(A \pm B) = \cos A \cos B \mp \sin A \sin B \qquad (7)$$

By using Eq. (7), (6) can be rewritten by:

$$Err_h = \sqrt{2}\ G\sin\theta_h \qquad (8)$$

The relationship between solar irradiation and short circuit current for west (I_{WS}) or east (I_{ES}) small PV module that is used as photo sensor is given by:

$$G_{WS} = 21000 * I_{WS} \qquad (9.a)$$
$$G_{ES} = 21000 * I_{ES} \qquad (9.b)$$

where G_{WS}, G_{ES} are irradiation at west and east photo sensors respectively.
And the relationship between I_{WS} and voltage applied to ADC0808 (V_{WS}) for west photo sensor is given by:

$$I_{WS} = \frac{V_{WS}}{49.5\Omega} \qquad (10.a)$$

Also, the relationship between I_{ES} and voltage applied to ADC0808 (V_{ES}) for east photo sensor is given by:

$$I_{ES} = \frac{V_{ES}}{49.5\Omega} \qquad (10.b)$$

Since FPGA reads analog input as quantization level, therefore the conversation formula from voltage (V) to quantization level (L) is given as:

$$V_{WS} = L_{WS} * \frac{3.27}{255} \qquad (11.a)$$

$$V_{ES} = L_{ES} * \frac{3.27}{255} \qquad (11.b)$$

where L_{WS} and L_{ES} are the voltage applied to ADC0808 which measured quantization level for west and east photo sensors respectively, 3.27V is reference voltage for ADC 0808 and 255 comes from its resolution is 8 bit.

By using Equations (8-11), the horizontal misalignment error (E_h) that FPGA computes it as quantization level is given as:

$$E_h = 0.26 \, G \sin \theta_h \qquad (12)$$

However, the Eq. (12) has been compared with the extracted equation from experimental data which has been collected and curve fitting is given by:

$$E_h = 0.2365 \, G \sin \theta_h \qquad (13)$$

The Eq. (13) is the basic equation which is adopted, although it is similar to the Eq. (12).

Since photo sensors system for polar axis and tilt axis are identical, the Eq. (13) can be written for the vertical misalignment error (E_v) by:

$$E_v = 0.2365 \, G \sin \theta_v \qquad (14)$$

where θ_v is the vertical misalignment angle and FPGA computes E_v as quantization level.

Each sensor is mounted the tilted surface by angle 45° in order to search the sun at dawn or after cloud passing. On other hand, the gain or sensitivity reading for sun tracker sensors is good as shown in Eq. (13).

IV. ENERGY GAIN IN THE PROPOSED SUN TRACKING SYSTEM

Solar tracker can be built by using one axis, and for higher precision, dual axis sun tracker. For a dual axis sun tracker, two types are tilt-polar tracking is used and azimuth-elevation tracking.

The relationship between the power gain and the misalignment angle θ is given by [1]:

$$P = P_{\max} \cos \theta \qquad (15)$$

when   θ is zero, that means, the sunlight is perpendicular to the panel, then the sun tracker captures to the maximum power .

The power losses (P_{losses}) due to the misalignment angle θ is can be written by:

$$P_{losses} = P_{\max} (1 - \cos \theta) \qquad (16)$$

For example, sun tracker that has accuracies of ± 10° can capture greater than 98.5% of the power generated by the direct beam of the sunlight as well as the diffuse light.

There are trade off, in the sun tracker design, between reduction of the power losses due to the misalignment the panel to the sun, and reduction of the losses power due to energy consumption in the motors and reduction lifetime of the sun tracker.

The criterion adopted in the design assumes that the ratio losses power from maximum power do not exceed to 1% under 1000 W/m^2 irradiation and 25 ^{o}C temperature. When applying this ratio in Eq. (16), the maximum misalignment angle θ is $\pm 8.11^o$.

It can be seen in Figure 12 that the adjacent side (n) of the angles θ, θ_h and θ_v is common and square the hypotenuse (c opposite side for θ) is equal to the sum of the squares of other two sides (a and b opposite sides of the angles θ_h and θ_v respectively) based on Pythagoras's theorem, so

$$\tan \theta = \sqrt{\tan^2 \theta_h + \tan^2 \theta_v} \qquad (17)$$

Since polar axis design is identical with tilted axis design, so the maximum θ_h is equal to the maximum θ_v and is $\pm 5.75^o$.

By using Eq. (13) and (14) to calculate the maximum horizontal and vertical misalignment error in FPGA is 23 for each one, whereas is equivalent to 5.75^o angle. This calculation takes into the account at irradiation is 1000 W/m^2.

To compute the interval that motor of the polar axis operates, the hour angle varies 1° every 4 minutes as shown in Eq. (2). So, the time interval is

$$5.75^o * \frac{4 \; Minutes}{1^o} = 23 \; Minutes$$

This interval is appropriate for the balancing between power losses and energy consumption in the motors and reduction lifetime of the sun tracker.

Also, to compute the interval that motor of the tilt axis operates, the declination angle is calculated according to Eq. (1). For example at 21 March, the time interval is about 14 day.

Hence, it is concluded that the proposed tilt-polar tracking system spends small energy since motor of the tilt axis motor operates in large time interval with keeping on energy gain for the sun tracker.

V.   ARCHITECTURE   OF   ADAPTIVE NEURO   FUZZY   INFERENCE   SYSTEM (ANFIS)

It is a process for mapping of given data set from multi inputs or single input to a single output which is achieved by the fuzzy logic and the artificial neuro networks. Using a given input–output data set, ANFIS constructs a Fuzzy Inference System (FIS) whose fuzzy membership function parameters are adjusted using hybrid learning method includes back propagation and least square algorithms [10].

For simplicity, it is assumed that the fuzzy inference system has two inputs x and y and one output z. The common rules set with fuzzy if-then rules are given as [11]:

Rule 1: If x is A_1 and y is B_1, then $f_1 = p_1x + q_1y + r_1$,

Rule 2: If x is A_2 and y is B_2, then $f_2 = p_2x + q_2y + r_2$.

This rule is a first order Sugeno fuzzy model.

ANFIS architecture for this model is indicated in Figure 14 , where nodes of the same layer have similar functions, as described next. (Here, the output of the ith node in layer l is denoted as $O_{l,i}$).
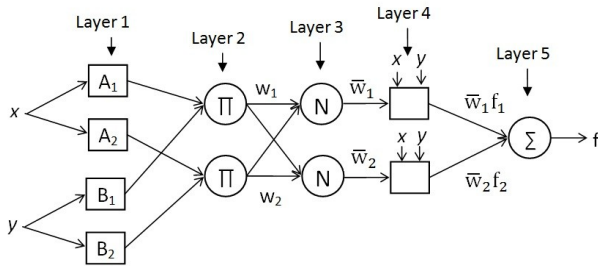

Figure 15: ANFIS architecture for the Sugeno fuzzy model

Layer 1: Every node i in this layer is an adaptive node with a node function

$$O_{1,i} = \mu_{Ai}(x), \qquad \text{for } i=1,2, \text{ or}$$

$$O_{1,i} = \mu_{Bi-2}(y) \qquad \text{for } i=3,4,$$

where y (or x) is the input to node i and A_i (or B_{i-2}) is a linguistic value (such as "hot" or "cold") associated with this node. In other words, $O_{1,i}$ is the membership grade of a fuzzy set A ($=A_1$, A_2 , B_1 or B_2) and it specifies the degree to which the given input x (or y) satisfies the quantifier A. The membership function for A can be any appropriate parameterized membership function, such as the generalized triangle function:

$$\mu_{Ai}(x) = \begin{cases} 0, & x \leq a_i \\ \dfrac{x - a_i}{b_i - a_i}, & a_i \leq x \leq b_i \\ \dfrac{c_i - x}{c_i - b_i}, & b_i \leq x \leq c_i \\ 0, & x \geq c_i \end{cases}$$

where $(a_i,\ b_i,\ c_i)$ is the parameter set. The parameters a_i and c_i locate the feet of the triangle and the parameter b_i locates the peak.

As the values of these parameters change, the triangle -shaped function varies accordingly, thus exhibiting various forms of membership function for fuzzy set A. Parameters in this layer are referred to as premise parameters.

Layer 2::Every node in this layer is a fixed node labeled Π, whose output is the product of all the incoming signals

$$O_{2,i} = w_i = \mu_{Ai}(x)\mu_{Bi}(y), \qquad i=1,2$$

Each node output represents the firing strength of a rule. In general, any other T-norm operators that perform fuzzy AND can be used as the node function in this layer.

Layer 3 : Every node in this layer is a fixed node labeled N. The ith node calculates the ratio of the ith rule's firing strength to the sum of all rules' firing strengths:

$$O_{3,i} = \overline{w}_i = \frac{w_i}{w_1 + w_2}, \qquad \text{for } i=1,2.$$

Outputs of this layer are called normalized firing strengths.

Layer 4: Every node i in this layer is an adaptive node with a node function:

$$O_{4,i} = \overline{w}_i f_i = \overline{w}_i(p_i x + q_i y + r_i)$$

where $\overline{w}_i$ is a normalized firing strength from layer 3 and $\{p_i, q_i, r_i\}$ is the parameter set of this node. Parameters in this layer are referred to as consequent parameters.

Layer 5: The single node in this layer is a fixed node labeled ∑, which computes the overall output as the summation of all incoming signals:

$$\text{Overall output} = O_5 = \sum_i \overline{w_i} f_i = \frac{\sum_i w_i f_i}{\sum_i w_i}$$

Thus, an adaptive network has been constructed. It is functionally equivalent to a Sugeno fuzzy model. Note that the structure of this ANFIS is not unique, layers 3 and 4 can be combined to obtain an equivalent with only four layers, by the same token, the weight normalization can be achieved at the last layer as shown in Figure 15.
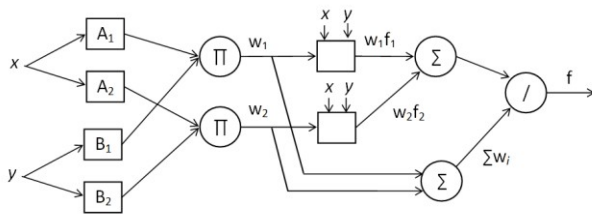
Figure 15: ANFIS architecture for the Sugeno fuzzy model, where weight normalization is performed at very last layer

VI. DESIGN AND IMPLEMENTATION NEURO-FUZZY CONTROLLER FOR THE SUN TRACKING SYSTEM

The neuro-fuzzy controller design based on zero order Sugeno fuzzy model which is indicated in Figure 15, because it contains one division operation only, hence it requires few FPGA resources (logic elements and etc). The neuro-fuzzy controller has two input variables which are: error and the error summation, and one output feeding to the motor driver.

For ease of implementation and saving the FPGA resources, it has been chosen three triangle memberships for each input due to its simple formulas and computational efficiency. Figures (16-17) illustrate the fuzzy set of the error input and the error summation respectively. Also, it has been chosen arbitrarily the nine output membership functions that are singletons and their parameters are (-2,-1,0,-1,0,1,0,1,2) from membership function 1 to 9 respectively.
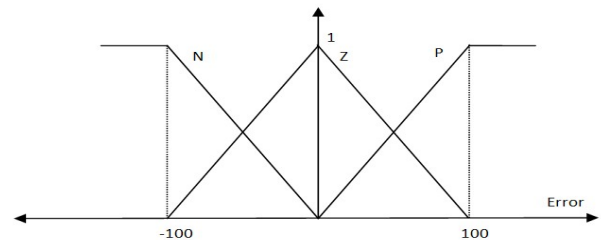

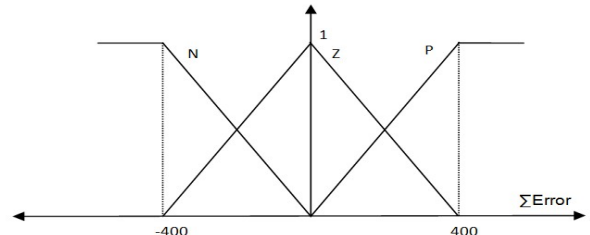Figure 16: The error fuzzy set

Figure 17: The error summation fuzzy set

To design robust controller under presence of the disturbances, it is necessary to train the controller under these circumstances. After set the date, the controller has been trained by offline Matlab tool box. The training is apply into the consequence parameters, which will be (-2,0.27, 0,-1.51,0,1.51 ,0,-0.27,2) from membership function 1 to 9 respectively.

Figure 18 shows the fuzzy rule surface viewer before and after the training phase.
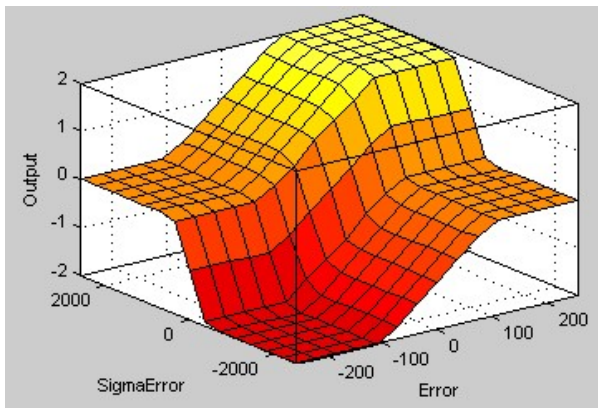
VII. SIMULATION AND RESULTS OF THE NEURO-FUZZY CONTROLLER BASED SUN TRACKING SYSTEM

Figure 19 indicates the Simulink block diagram for the proposed neuro- fuzzy controller based sun tracking system with optical sensors and linear actuator.
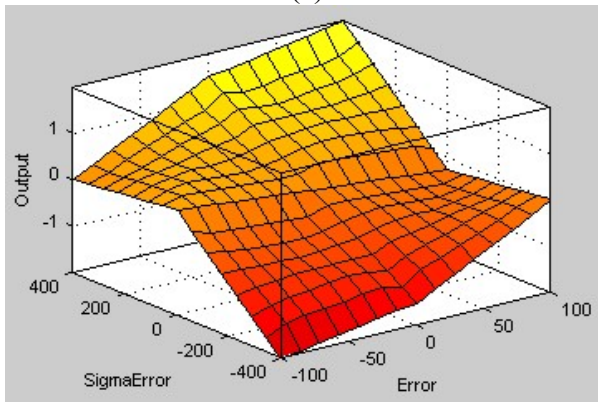
The controller has been tested using Matlab/Simulink for one hour under 1000 W/m^2 irradiation. The daily sun motion can be represented by a ramp source block whose slope equals to (1°/240s) since the sun position varies 1° every 240 second; and initial output equals to zero degree.

Figure 20 indicates also the horizontal misalignment error (E_h) practically measured by quantization level (0-255) during 10 minutes. This Figure reveals effect the disturbances on outputs of the optical sensors as shot noise.

The shot noise may be simulated as two pulse generators. It added to the optical sensors output since it represents a measurement noise.

about 22 minutes due to sensitivity of the optical sensors system to a variation of the irradiation.
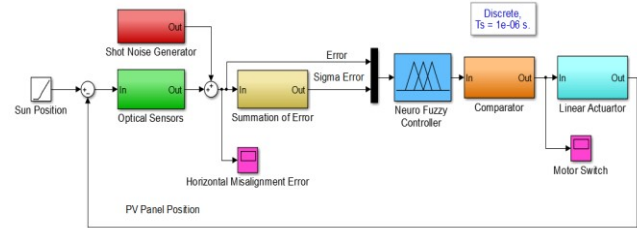

Figure 19: Simulation of the neuro-fuzzy controller based the sun tracking system using Matlab/Simulink
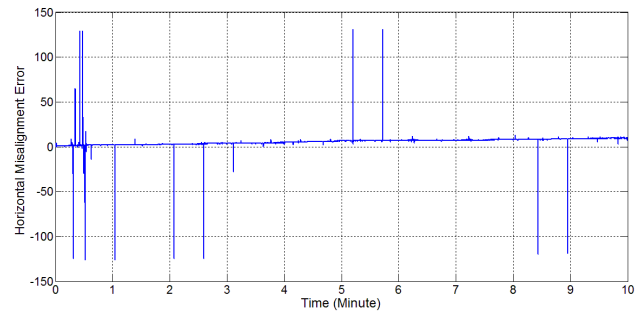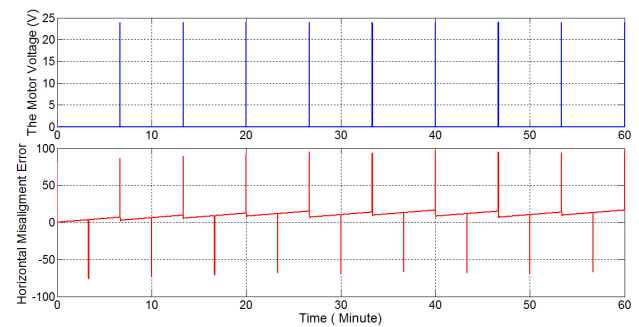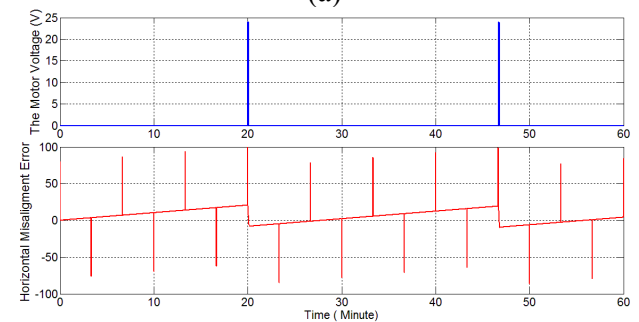

Figure 20: The horizontal misalignment error practically measured by quantization level (0-255) during 10 minutes

(a)

(b)

Figure 21: The simulated response of the neuro-fuzzy controller for the sun tracking system for one hour (a) before training (b) after training

(a)

(b)

Figure 18: Fuzzy rule surface viewer (a) before training (b) after training

The simulated response of the horizontal misalignment error (quantization level) and the motor switch are indicated in Figure 21. Figure 21 (a) indicates the simulated response of PI-like fuzzy controller (before training). Note that the controller is not robust against the disturbances where it is affected with positive pulses and is not affected negative pulses because the error summation always is positive (the sun always moves from the east to the west). So, interval of the motor switch is about 7 minutes. That mean, it does not corresponds to the design that is mentioned in section IV where interval of the motor switch would be 23 minutes under 1000 W/m^2 irradiation.

Figure 21 (b) indicates the simulated response of PI-like fuzzy controller (after training) or neuro-fuzzy controller. Note that the controller is so robust against the disturbances where it is not affected with positive or negative pulses. In addition, the simulated results approximately corresponds to the design that is mentioned in section IV, where interval of the motor switch is

VIII. ROBUSTNESS OF THE NEURO-FUZZY CONTROLLER FOR THE SUN TRACKING SYSTEM

For performance evaluation, the fuzzy logic and neuro-fuzzy controllers have been investigated by experimental tests.

Figure 22 indicates the practical response of the fuzzy logic controller (before training) during one hour in sunny day. Note that the number of the switching is 11 times which mean that the polar axis motor switches quickly.

Figure 23 indicates the practical response of the neuro-fuzzy controller (after training) during one hour in sunny day. Note that the number of the switching is 2, which means that the motor switches corresponds to the design that is mentioned in section IV where interval of the motor switch is about 23 minutes.

Figure 24 indicates the practical response of the neuro-fuzzy controller during one hour in partly cloudy day. Note that the controller performance is good and does not affect when passing the clouds. In contrast, sensitivity of the photo sensors decreases with decreasing the irradiation according to Eq. (13).
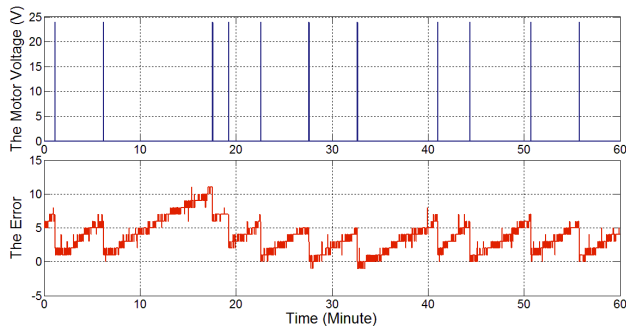

Figure 22: The practical response of the fuzzy logic controller (before training) during one hour in sunny day

For digital control, the sampling period (T_s) has been chosen as 1 second since the system contains the mechanical parts which have large time constant.

The error sum is a sum of the ten past error sample that should be stored. It is suitable to the admissible error angle is $\pm 5.75^{\circ}$ and the average angular speed of the panel is $1^{\circ}/s$.
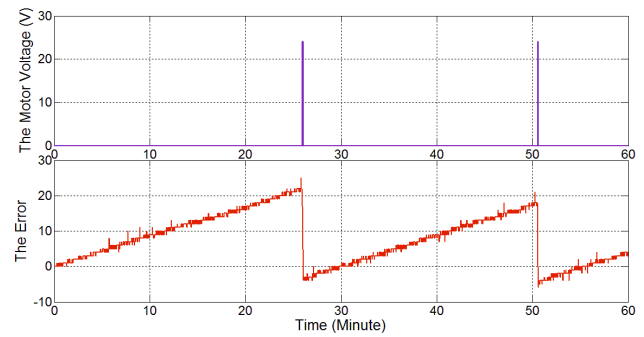

Figure 23: The practical response of the neuro-fuzzy controller (after training) during one hour in sunny day
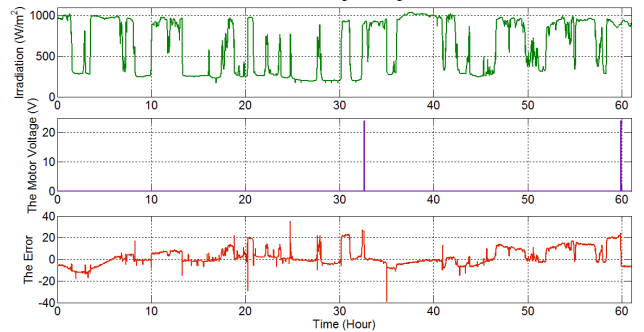

Figure 24: The practical response of the neuro-fuzzy controller after training during one hour in partly cloudy day

For comparison purpose, the conventional digital PI controller has been designed and implemented on the FPGA board with proportional gain (K_p) is 1 and integration gain (K_i) is 0.1. Figure 25 shows the practical response for PI controller during 15 minutes in sunny day. Note that the number of the switching is 12 and the motor rotates in two directions, from the east to the west or the reverse direction, although the sun apparently moves from the east to the west, that means that PI controller robustness is not good at presence of the disturbances.

In summary, the proposed neuro-fuzzy controller is more robust than the fuzzy logic controller and the PI controller since it has been trained to operate with these disturbances.

IX. EXPERMINTAL RESULTS

The experimental data have been measured every 30 minutes. Figure 26 shows the plot of power which is generated by SR-60S PV module throughout days when start from 13 to 15 January for the same load.
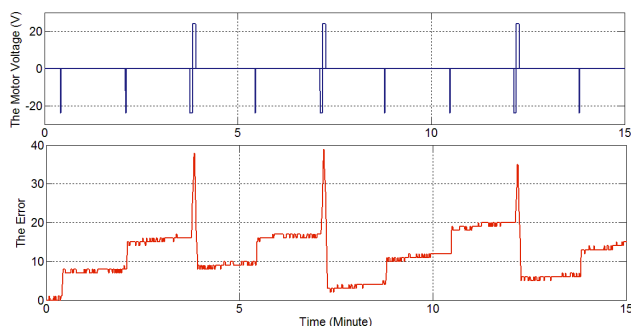
Figure 25: The practical response of PI controller during 15 minutes in sunny day

Table 1 shows these data at fixed angle panel, one and dual axis sun tracker .

Table 1
Experimental Results of Fixed Angle Panel, One and Dual Axis Sun trackers throughout Sunny Day

Time of day	The power output (W) at fixed angle panel	The power output (W) at one axis sun tracker	The power output (W) at dual axis sun tracker
7:00	0.04	0.04	0.13
7:30	0.97	0.69	0.97
8:00	17.07	34.34	36.47
8:30	20.29	43.62	46.81
9:00	26.23	48.34	52.5
9:30	34.56	48.41	53.95
10:00	39.36	47.89	56.32
10:30	44.37	50.76	57.65
11:00	46.51	49.59	57.71
11:30	48.09	50.8	57.87
12:00	50.15	52.46	58.54
12:30	48.92	51.55	57.35
13:00	47.03	52.14	58.54
13:30	44.18	51.26	56.56
14:00	40.39	50.22	55.09
14:30	34.76	49.06	52.45
15:00	27.41	48.74	48.69
15:30	20.39	45.47	43.43
16:00	12.69	40	37.31
16:30	2.02	28.6	23.57
17:00	0.04	0.13	0.13
Sum	605.47	844.11	912.04

Reference [12] author recommends that fixed angle PV panel tilted at an angle equals to the latitude in which it is situated and faced toward the south if it lies on the northern hemisphere and vice versa.

At fixed angle PV panel and one axis sun tracker tests, the module surface is tilted at 31° respect to the earth and situated and faced toward the south since the module lies on 31° North latitude.

From Table 1, the energy gain for one axis sun tracker can be calculated by:

$$\text{Energy gain}=\frac{844.11-605.47}{605.47}\ 100\ \%=39.4\ \%$$
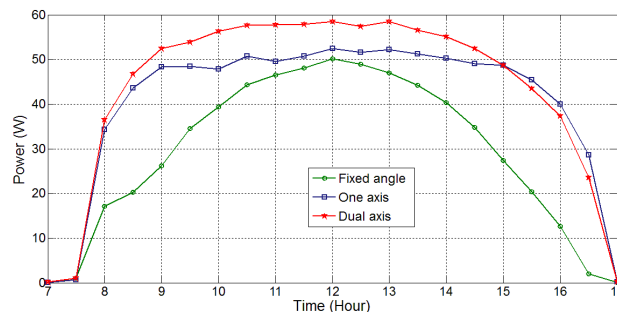

Figure 26: Power comparison at fixed angle panel, one and dual axis sun tracker

while the energy gain for dual axis sun tracker depends on the date of the data acquisition (13 January), which can be calculated by:

$$\text{Energy gain}=\frac{912.04-605.47}{605.47}\ 100\ \%=50.6\ \%$$

In other word, the one axis sun tracker can collect 39.4% more energy than fixed angle panel, whilst the dual axis sun tracker can collect 50.6% more energy than fixed angle panel.

The energy gain between dual and one axis sun tracker may be calculated by:

$$\text{Energy gain}=\frac{912.04-844.11}{844.11}\ 100\ \%=8\ \%$$

That mean that dual axis sun tracker can collect 8 % more energy than one axis sun tracker.

From the experimental results which have been obtained through different days, it is concluded that the dual axis sun tracker controller has a good performance to track the sun automatically and it is efficient in energy collection where it can collect up 50% more energy than what a fixed panel collects.

X. CONCLUSION
In this paper, neuro-fuzzy based dual axis (tilt-polar) sun tracker has been designed and implemented using Altera EP4CE6E22C8N

FPGA board to enhance the efficiency of the PV module by tracking the sun.

The neuro-fuzzy controller design takes into account, the balance between reduction of the losses power due to the misalignment the panel to the sun, and reduction of the losses power due to energy consumption in the motors and reduction lifetime of the sun tracker.

The proposed controller has been trained offline using Matlab tool box to operate with the disturbances. The experimental results reveal that the proposed neuro-fuzzy controller is more robust and effective than the fuzzy logic and the PI controllers.

The proposed controller can boost energy gain effectively, where the experimental results reveal that dual axis sun tracker power can collect 50.6% more daily power than fixed angle panel. Whilst one axis sun tracker power can collect 39.4 % more daily power than fixed angle panel. Hence, the proposed dual axis sun tracker can collect 8 % more daily power than one axis sun tracker.

REFERENCES

[1] H. Mousazadeh, A. Keyhani, A. Javadi, H. Mobli, K. Abrinia and A. Sharifi, "A review of principle and sun-tracking methods for maximizing solar systems output", *Renewable and Sustainable Energy Reviews*, Volume 13, Issue 8, October 2009, Pages (1800–1818).

[2] H. Yousef, "Design and implementation of a fuzzy logic computer-controlled sun tracking system", *Proceedings of the IEEE International Symposium on Industrial Electronics,* Volume 3, 12-16, July 1999, Pages (1030 – 1034).

[3] M. EL-Moghany, "Sun and Maximum Power Point Tracking in Solar Array Systems Using Fuzzy Controllers via FPGA", Master Thesis, *Islamic University-Gaza*, 2011.

[4] K. ElNounou, "Design of GA- Sugeno Fuzzy Controller for Maximum Power Point And Sun Tracking in Solar Array Systems", Master Thesis, *Islamic University-Gaza*, 2013.

[5] H. Akkar and Y. Abid, "Design of Intelligent Controller for Solar Tracking System Based on FPGA", *Eng. & Tech. Journal,* Volume 33, Part (A), NO.1, 2015, Pages (114-128).

[6] S. Szokolay, "Solar Geometry", Passive and Low Energy Architecture International notes, Note1, second revised edition, 2007.

[7] S. Hyder, D. Kanth, C. Chandrasekhar, E. Sammaiah, "Field Programmable Gate Array Implementation Technology", *International Journal of Engineering and Advanced Technology*, ISSN: 2249 – 8958, Volume-2, Issue-1, October 2012, Pages (25-29).

[8] Altera Corporation, "Cyclone IV FPGA Device Family Overview", Cyclone IV Device Handbook, Volume 1, April 2014.

[9] National Semiconductor Corporation, "ADC0808/ADC0809 8-Bit μP Compatible A/D Converters with 8-Channel Multiplexer", May 2006.

[10] S. Hakim and H. Abdul Razak, "Damage Identification Using Experimental Modal Analysis and Adaptive Neuro-Fuzzy Interface System (ANFIS) ", Topics in Modal Analysis I, Volume 5, Conference Proceedings of the Society for Experimental Mechanics Series 30, 2012, Pages (399-404).

[11] JSR Jang, "Neuro-fuzzy and soft computing", Prentice-Hall, 1997.

[12] International Renewable Energy Agency, "Renewable Energy Technologies: Cost Analysis Series", Volume 1:power sector, Issue 4/5:Solar Photovoltaics, June 2012.